Cu^{2+} binding triggers αBoPrP assembly into insoluble laminar polymers

Reinerio González-Iglesias[a], Gema Elvira[a], José A. Rodríguez-Navarro[a], Marisela Vélez[b], Miguel Calero[c], María A. Pajares[d], María Gasset[a,*]

[a] *Instituto Química-Física 'Rocasolano', CSIC, Serrano 119, E-28006 Madrid, Spain*
[b] *Instituto Nicolás Cabrera, Facultad de Ciencias, Universidad Autónoma de Madrid, E-28049 Madrid, Spain*
[c] *Centro Nacional de Microbiología, Instituto de Salud Carlos III, Majadahonda, E-28220 Madrid, Spain*
[d] *Instituto Investigaciones Biomédicas 'Alberto Sols', CSIC-UAM, Arturo Duperier 4, 28029 Madrid, Spain*

Received 12 November 2003; accepted 20 November 2003

First published online 3 December 2003

Edited by Thomas L. James

Abstract **Cu^{2+} binding is so far the best characterized property of the prion protein. This interaction has been mapped to the N-terminal domain of the prion protein where multiple His residues occur largely embedded within the repetitive PHGGGWGQ sequence known as octarepeats. When Cu^{2+} interaction is studied using a solution of full-length bovine prion protein containing six octarepeats at protein concentrations above 25 μM, a drastic increase in solution turbidity is observed due to the formation of insoluble cation–protein complexes that appear as bidimensional polymer meshes. These bidimensional meshes consist of a single layer of protein molecules crosslinked by Cu^{2+} cations. Polymer formation is a cooperative process that proceeds by nucleation of protein molecules with a Cu^{2+} site occupancy of above 2. These results support the hypothesis that the N-terminal domain of prion protein is a ligand binding module that promotes crosslinked assembly, and suggest the existence of inter-repeat Cu^{2+} sites.**

Key words: Prion protein; Protein assembly; Intermolecular cation binding; Cu^{2+}–prion protein interaction

1. Introduction

PrP^C, the cellular prion protein, has become a key molecule in brain for the understanding of the lethal neurodegenerative disorders known as transmissible spongiform encephalopathies [1,2]. In these diseases, PrP^C is thought to undergo a major conformational transition that promotes its perpetuation in vivo as a complex, structurally defined aggregate [2–4]. This transition is characterized by the stabilization of alternative conformers with a higher proportion of β-sheet structure relative to the normal physiological form. These conformational changes, which occur in the C-terminal globular domain, distort the solubility pattern, confer aggregation properties and impair the normal clearance rate of the protein [2,4–7].

PrP^C is a Cu^{2+} binding protein and its function in cation homeostasis is impaired on its conversion to PrP^{Sc} [8–25]. Cu^{2+} interaction has been mapped mainly at the N-terminal region, which contains tandem repeats of the sequence PHGGGWGQ known as octarepeats [11–17,20,25]. In the absence of this cation this segment is randomly structured and highly flexible but it becomes structurally constrained upon metal chelation [15,20,25–27]. Each His residue of the octarepeat segment has the capacity to harbor a Cu^{2+} atom in a cooperative process characterized by affinity constants that lie in the femto- to micromolar range and Hill coefficients of 2.6–4.2 [19,20,22,23,28]. In addition to the octarepeat region, full-length PrP contains two other Cu^{2+} binding sites which involve His residues located on either side of the amyloid region [19,25,28].

Most studies on the interaction between PrP^C-like folded PrP (αPrP) and Cu^{2+} in solution have been performed using low protein concentrations, and they were focused on intramolecular Cu^{2+} binding [22,25]. However, the multiplicity of sites in the αPrP molecules and their location in flexible solvent-exposed regions together with the propensity of Cu^{2+} to form penta-coordinated complexes allows, in principle, the formation of intermolecular complexes. Evidence for the participation of αPrP in Cu^{2+}-mediated heteropolymer associations, such as with chromatographic matrices and glycosaminoglycans [8,29–31], are available but the capacity of Cu^{2+} to promote αPrP self-association has never been inspected. Using turbidity and solubility measurements, we have found that Cu^{2+} binding triggers the formation of polymers of cation-bound full-length bovine PrP containing six octarepeats (αBoPrP(24–242)) in a process that depends on both the protein concentration and the Cu^{2+} site occupancy. The formation of insoluble Cu^{2+}–αBoPrP(24–242) complexes requires binding of more than 2 Cu^{2+} equivalents. This allows the crosslinking of different protein molecules into amorphous bidimensional meshes stabilized by side contacts and sensitive to proteolytic degradation. The results that we have obtained support the role of the N-terminal domain of αPrP as a polymerization domain whose activity requires ligand binding, and points to the existence of alternative and as yet undescribed Cu^{2+} site geometries employed in this activity.

2. Materials and methods

2.1. αBoPrP(24–242) production

BoPrP(24–242) was expressed from pET11a plasmids in *Escherichia coli* (BL21-DE3) and refolded after disulfide bond formation as pre-

*Corresponding author. Fax: (34)-915-642 431.
E-mail address: mgasset@iqfr.csic.es (M. Gasset).

Abbreviations: BoPrP(24–242), full-length bovine prion protein containing six octarepeats ($MK^{25}RPK$-...-$G^{240}AS$); αPrP, prion protein-C-like folded prion protein

0014-5793/03/$30.00
doi:10.1016/S0014-5793(03)01397-8

viously described [30]. Before use, αBoPrP(24–242) was extensively dialyzed against 20 mM MES pH 6.5, 50 mM NaCl and 0.03% NaN_3 to ensure the removal of citrate and cleared by centrifugation at 10 000 × *g* for 30 min at 4°C. When required, protein solutions were concentrated by ultrafiltration using YM-10 membranes (Amicon, Millipore) and stored at −20°C. The protein concentration was determined spectrophotometrically in 6 M GdnCl (Pierce) using a molar extinction coefficient ε_{280} of 62 280 M^{-1} cm^{-1}.

2.2. Cation solutions

Cu^{2+}, Zn^{2+} and Mn^{2+} solutions were freshly prepared by dissolving the required amount of the corresponding sulfate salts (Merck) in boiled MilliQ water and then diluted into freshly N_2-bubbled solutions. Dilution of cation stock solutions into either buffer or protein solutions occurred with no observable pH change. Cu^{2+} concentrations were determined spectrophotometrically [32] using a calibration curve verified by inductively coupled plasma optical emission spectrometry.

2.3. Turbidity measurements

The changes in protein solution turbidity were followed by measuring the increase in the absorbance at 360 nm in an Ultrospec 3000pro spectrophotometer (Amersham Pharmacia Biotech) using a thermostatted eight cell unit holder. Measurements were performed at 25°C using 0.1, 0.5 and 1 cm pathlength cuvettes. Samples were allowed to equilibrate for 10 min before Cu^{2+} addition. Absorbance (*A*) readings were corrected for buffer contribution and then converted to optical density (OD) for normalization of data to 1 cm pathlength.

2.4. Solubility determination

αBoPrP(24–242) solutions in 20 mM MES pH 6.5 containing 50 mM NaCl and 0.03% NaN_3 at varying concentrations were incubated in the absence or presence of 1, 2, 3, 5, and 10 Cu^{2+} equivalents for 10 min at 25°C. After removing aliquots for the determination of total cation and protein content (T), the reaction mixtures were centrifuged at 10 000 × *g* for 30 min at 4°C, and separated into pellet (P) and supernatant (S) fractions. The protein concentrations in the soluble and pellet fractions were determined either spectrophotometrically in 6 M GdnCl (Pierce) using a molar extinction coefficient ε_{280} of 62 280 M^{-1} cm^{-1} or by quantitative dot-blot analysis. For dot-blot analysis, samples were spotted in triplicate onto nitrocellulose membrane mounted on a dot-blot cassette (Bio-Rad) and then denatured with 6 M GdnCl. After extensive washes, the membrane was blocked with 3% non-fat dry milk in TBST (10 mM Tris–HCl pH 7.4, 150 mM NaCl, 0.05% Tween 20) and then incubated with monoclonal antibody 6H4. Detection was performed using a horseradish peroxidase-conjugated secondary antibody (Sigma) and ChemiLucent reagent (Chemicon). Signal detection and analysis were carried out with the ChemiDoc Bio-Rad system and the Quantity One software. For pellet concentration, protein and cation contents were referenced to the total volume.

2.5. Atomic force microscopy (AFM)

Pellets from αBoPrP(24–242) solutions treated with 3 Cu^{2+} equivalents were dispersed in 20 mM MES pH 6.5 containing 50 mM NaCl and 0.03% NaN_3 at 1 mg/ml protein concentration. Typically, 50 μl of the freshly prepared resuspension was deposited onto a mica surface that had just been freshly cleaved and immersed in 2 M KCl, allowed to adsorb for 1 h and then extensively washed with buffer. Images were taken with an atomic force microscope (Nanotec Electrónica, Madrid, Spain) operated in contact or jump mode, with silicon nitride tips with a force constant of 0.12 N/m (DI Instruments). The samples were maintained in buffer solution during imaging.

3. Results

3.1. Cu^{2+} induces the aggregation of αBoPrP(24–242)

Addition of increasing molar equivalents of Cu^{2+} ions to solutions of αBoPrP(24–242) induces the appearance of turbidity that can be monitored by measuring the absorbance at 360 nm. This turbidity clarifies upon centrifugation at 10 000 × *g* for 30 min, yielding transparent supernatants with decreased protein concentration indicating the formation of αBoPrP(24–242) insoluble aggregates. Kinetic traces from 68 μM αBoPrP(24–242) solutions at increasing Cu^{2+} equivalences are shown in Fig. 1. The increases in A_{360} are specifically related to Cu^{2+} interaction since its replacement by Zn^{2+} or Mn^{2+} does not modify the initial A_{360} reading. Addition of Cu^{2+} in the absence of protein does not change the initial reading and when Cu^{2+} is added as a 1:2 complex with a chelator (nitrilotetraacetate and citrate), the increase in ΔA_{360} shifts to a higher total concentration of Cu^{2+} concomitant with the pH-corrected complex stability constant (Fig.

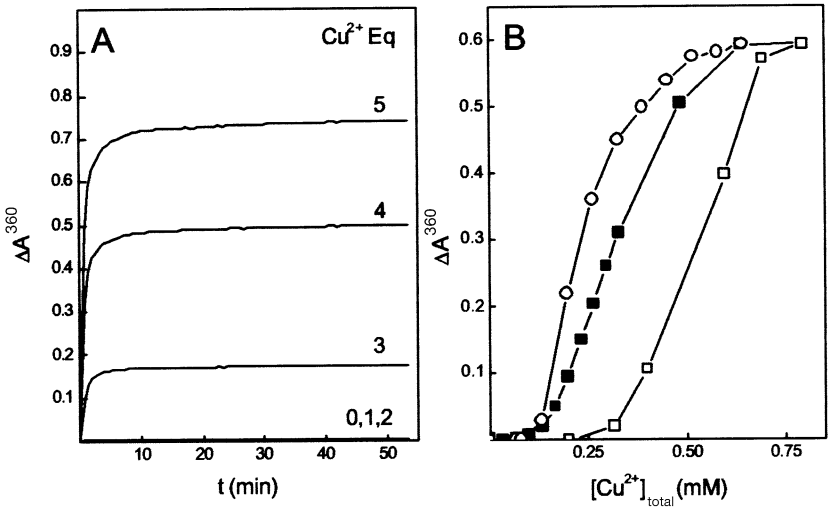

Fig. 1. Cu^{2+}-induced aggregation of αBoPrP followed by turbidity measurements. A: αBoPrP(24–242) solutions (68 μM) in 20 mM MES pH 6.5 containing 50 mM NaCl and 0.03% NaN_3 were placed in cuvettes of 0.1 or 0.5 cm pathlength and equilibrated for 5 min previous to the addition of 0, 1, 2, 3, 4 or 5 Cu^{2+} equivalents and their absorbance at 360 nm measured as a function of time in 0.1 cm pathlength cells without stirring. Displayed traces were corrected by the contribution of the corresponding protein-free baselines. B: Effect of Cu^{2+} availability on the turbidity increase. αBoPrP(24–242) solutions (68 μM) in 20 mM MES pH 6.5 containing 50 mM NaCl and 0.03% NaN_3 were titrated stepwise with Cu^{2+} in the absence (○) or presence of two-fold molar excess of citrate (■) or nitrilotetraacetate (□) carriers. Before taking the A_{360} readings in 0.1 cm cuvettes, samples were allowed to equilibrate for 15 min and then vortexed by double inversion.

1B) [33]. The appearance of turbidity is not prevented by the presence of non-ionic detergents such as Tween 20 and Brij 96-V below and above the micellar concentration (data not shown). These observations exclude the participation of either side reactions arising from the intrinsic instability of Cu^{2+} solutions at the working pH, or any Cu^{2+}-induced increase on the hydrophobicity of the protein surface in contributing to the observed turbidity in the Cu^{2+}-induced protein aggregation event.

The time dependence of the increase in the A_{360} readings showed that the changes occurred rapidly and the maximum was attained in less than 5 min (Fig. 1A). This pattern was conserved for different protein batches excluding artifacts stemming from conformational heterogeneities and the presence of undesired protein covalent modifications [34]. For a fixed protein concentration (68 μM) increasing the Cu^{2+} equivalents had no significant effect on the initial slope but altered the maximum A_{360} (Fig. 1A). Importantly, the maximum A_{360} remained constant over a period of time long enough to exclude fast reorganization events that would clear the optical path. Comparison of steady-state values from endpoint and stepwise Cu^{2+} titrations (Fig. 1A,B) showed differences in the ΔA_{360} and in the dependence on increasing Cu^{2+} saturation that suggest distinct final states differing in either concentration, size or both. In addition, once reached the maximum value of A_{360} dilution of the samples from 68 μM to 42.5 μM protein concentration caused a reduction in the A_{360} that was proportional to the dilution factor (data not shown), indicating the lack of reversibility over the time scale employed. This observation indicated that the Cu^{2+}-induced aggregation is kinetically favored and its evolution, if any, to a thermodynamically more favored state occurs would be a very slow process.

3.2. αBoPrP(24–242) in complex with Cu^{2+} is the aggregating species

To get insight into the nature of the aggregating species we performed a quantitative analysis of the composition of the pellet fractions obtained from a 30 min centrifugation at 10 000 × *g* of αBoPrP(24–242) solutions after the addition of increasing equivalents of Cu^{2+} (Fig. 2A). For 42.5 μM αBoPrP(24–242) the insoluble fraction contains both protein and Cu^{2+} and becomes enriched in both components as the number of added Cu^{2+} equivalents increases. It must be stressed that in the absence of the protein, 87% of the Cu^{2+} remains in solution up to the concentration corresponding to 10 equivalents excluding artifacts arising from possible Cu^{2+} instability except for the samples prepared at 10-fold molar excess of the cation. Therefore, this result shows that the aggregating species is the Cu^{2+}-bound protein.

Analysis of the Cu^{2+} saturation function of the insoluble fraction of αBoPrP(24–242) solutions at 42.5 and 85.2 μM initial concentrations reveals an increase in Cu^{2+} site occupancy as the total Cu^{2+} equivalents added increases (Fig. 2B), from 2.9 up to a value between 4 and 5. The lower limit of the saturation function indicates that saturation of at least half of the sites is critical for the formation of the insoluble aggregates. On the other hand, the upper limit of the saturation agrees with the 80% reduction in the theoretical maximum value of 6 due to pH effects [22,30]. Furthermore, for a total Cu^{2+} equivalence of 3, the saturation function of the insoluble phase becomes 2.9 ± 0.2 at protein concentrations

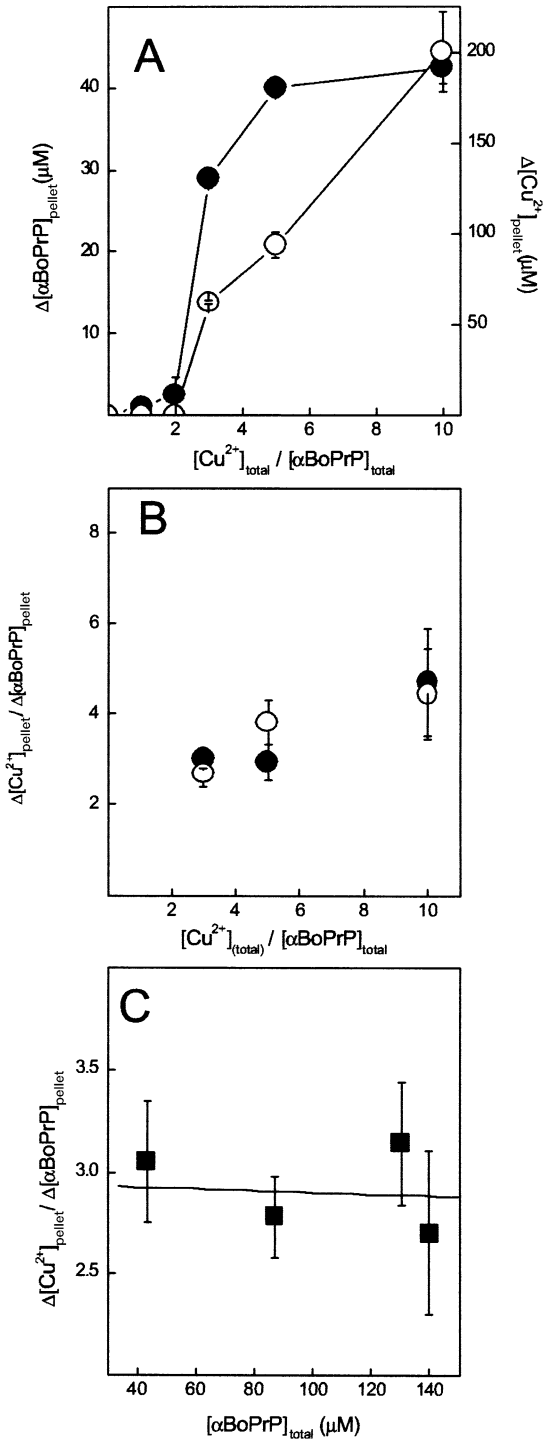

Fig. 2. Insoluble polymers are formed by αBoPrP(24–242) in complex with Cu^{2+}. A: Cu^{2+} (○) and αBoPrP(24–242) (●) concentrations in the pellet fractions of a 10 000 × *g* centrifugation for 30 min at 4°C of 42.5 μM protein solutions with increasing the addition of Cu^{2+} equivalents. Concentrations are referenced to the total initial volume. B: Dependence of Cu^{2+}–αBoPrP(24–242) composition on the number of added Cu^{2+} equivalents to 42.5 (●) and 85.2 (○) μM protein solutions. C: Variation of Cu^{2+} site occupancy in the insoluble αBoPrP(24–242) polymers with the initial concentration of protein:Cu^{2+} 1:3 mixtures. Displayed data are the average of three independent measurements, each with duplicate samples.

above 40 μM (Fig. 2C), indicating that the threshold occupancy of sites for the formation of insoluble aggregates is independent of the protein concentration.

3.3. The insoluble Cu^{2+}–αBoPrP(24–242) complexes are bidimensional meshes with lateral contacts among protein monomers

Formation of insoluble aggregates can be due to either intramolecular or intermolecular Cu^{2+} binding. If the loss of solubility upon Cu^{2+} binding was caused by a cation crosslinking event, then for a fixed Cu^{2+} concentration increasing αBoPrP(24–242) concentration would decrease the aggregation process since the excess of protein would reduce the probability of intermolecular bridging. For a constant concentration of Cu^{2+} of 129 μM, increasing αBoPrP(24–242) concentration from 43 to 86 μM reduces the percentage of protein precipitation from 39 (16.77 μM) to 10% (8.6 μM). Therefore, the aggregation process could be attributed to the formation of intermolecular Cu^{2+} crosslinks. To verify the existence of Cu^{2+}-induced contact sites we monitored the formation of the complexes by AFM. Protein–Cu^{2+} complexes prepared with 3 cation equivalents were isolated by centrifugation and transferred to 2 M KCl-treated freshly cleaved mica by dispersion in cation-depleted buffer. After 1 h of incubation and extensive washing, the inspection of the surface revealed an amorphous mesh of protein with a thickness of about 3 nm that corresponds to that expected for a single layer of a globular protein of about 23.5 kDa as in the case with αBoPrP(24–242) (Fig. 3). The extremely invariant thickness compared to the non-periodic bidimensional structure featured by holes and surface irregularities denoted a preferential orientation of the contacts among protein molecules in the plane parallel to the mica surface. Analysis of multiple samples and regions indicated large polydispersity in the direction parallel to the mica surface, with polymers displaying full widths at half height varying from 20 to 50 nm. These images agreed with that expected for a polymeric protein mesh organized preferentially in a layer sustained by Cu^{2+} staples among molecules.

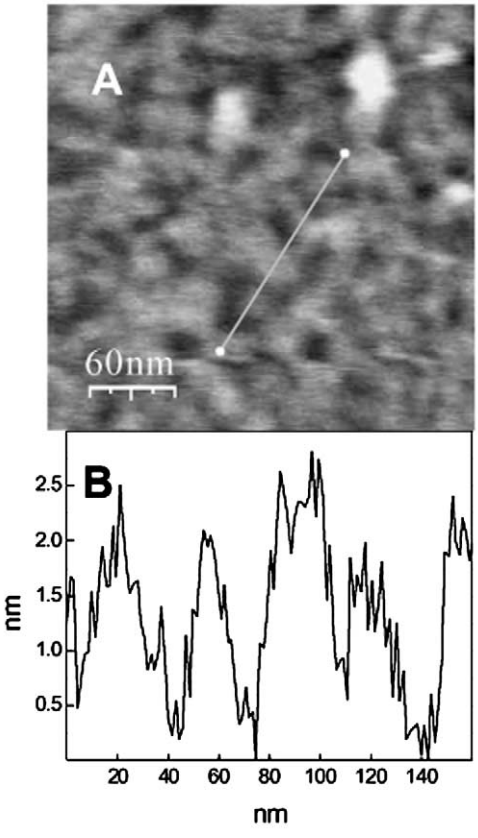

Fig. 3. AFM analysis of the morphology of Cu^{2+}-bound αBoPrP(24–242) insoluble complexes. A: AFM images of αBoPrP(24–242) polymers induced by Cu^{2+} binding. The white bar represents 200 nm and the height (black to white color scale) is 4 nm. B: Distance profile of a selected region (white bar) of the image shown in the top panel. The vertical axis corresponds to the thickness of the structures while the horizontal axis indicates the distance (related to the polymer width) of the selected segment.

3.4. Cu^{2+}-induced αBoPrP(24–242) aggregation is cooperative and follows a nucleated polymerization mechanism

Polymerization reactions that proceed by a condensation mechanism typically exhibit a cooperative dependence on the protomer condensation and a threshold or critical concentration for assembly. To determine whether Cu^{2+}-mediated αBoPrP(24–242) aggregation displays this characteristic, the relation of the maximum ΔOD_{360} as a function of αBoPrP(24–242) concentration in the presence of 3 Cu^{2+} equivalents was examined (Fig. 4A). The results show that the reaction is biphasic. The first phase is observed at αBoPrP(24–242) below 40 μM and consists of a slight increase in ΔOD_{360}. The second phase spans αBoPrP(24–242) concentrations in the 40–85 μM range and consists of a very steep rise on ΔOD_{360} with increasing protein concentration. Since for αBoPrP(23–232) concentrations above 40 μM the addition of 3 Cu^{2+} equivalents results in insoluble polymers containing 3 Cu^{2+} per protein mol (Fig. 4A), the solubility data can be used to explore the polymerization mechanism. Fig. 4B shows the analysis of the partition of αBoPrP(24–242) in the presence of 3 Cu^{2+} equivalents between the soluble and the insoluble phases as a function of αBoPrP(24–242) concentration. This partition pattern agrees with a nucleated polymerization with a critical concentration of 21 ± 4 μM in which the species undergoing the polymerization is the protein–Cu^{2+} complex. The existence of such an equilibrium process is further supported by the complete degradation of the Cu^{2+}–αBoPrP(24–242) polymers prepared at a 3:1 molar ratio, both in the absence and in the presence of 2% sodium sarcosinate, by proteinase K (Fig. 4C).

4. Discussion

The N-terminal domain of PrP has been recognized as a regulatory module in the overall metabolic process leading to the molecule's structural conversion, aggregation and deposition [35–38]. Among its functions, Cu^{2+} binding is the best known at the molecular level and has been described as the sequential acquisition of an individual Cu^{2+} cation by each of the PHGGGWGQ octarepeat motifs within the protein molecule with the subsequent folding of the polypeptide chain around the cation [13,15,17,20,25]. Additionally, Cu^{2+} binding also drives the participation of PrP through its N-terminal domain in hetero-association reactions [8,29–31], that support alternative geometries in Cu^{2+} sites. An immediate consequence of increasing the protein concentration regime used for Cu^{2+} binding studies is the occurrence of a protein polymerization event which agrees with previous studies with PrP^{C}

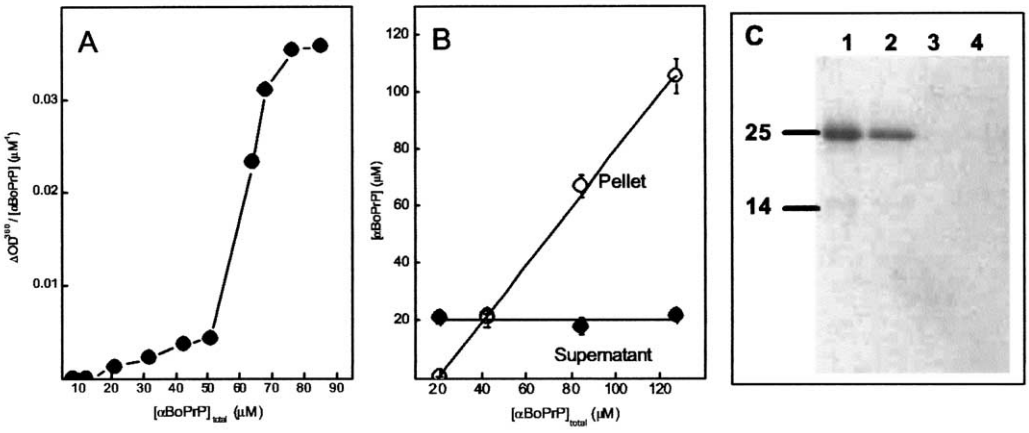

Fig. 4. Cu^{2+} binding-linked αBoPrP(24–242) polymerization is a cooperative and nucleated equilibrium process. A: Variation of the ΔOD_{360} as a function of protein concentration upon addition of 3 Cu^{2+} equivalents. Absorbance at 360 nm was measured in 0.1 cm optical pathlength cuvettes and then, after baseline subtraction, converted to OD and normalized to the protein concentration in μM units. B: Partition of αBoPrP(24–242) in the presence of 3 equivalents of Cu^{2+} between the soluble and pellet fractions as a function of protein concentration. C: Proteinase K sensitivity of Cu^{2+}–αBoPrP(24–242) polymers. Lanes correspond to: (1) Cu^{2+}–αBoPrP(24–242), (2) Cu^{2+}–αBoPrP(24–242) with 2% sodium sarcosinate, (3) proteinase K-digested Cu^{2+}–αBoPrP(24–242), and (4) proteinase K-digested Cu^{2+}–αBoPrP(24–242) with 2% sodium sarcosinate. Insoluble polymers isolated by centrifugation of αBoPrP(24–242) solutions treated with 3 Cu^{2+} equivalents were dispersed at 50 μM in 20 mM MES pH 6.5, 50 mM NaCl and 0.03% sodium azide in the absence and presence of 2% sodium sarcosinate (Sigma). Digestions were performed by incubation for 1 h at 37°C with 40 μg/ml proteinase K (Roche) and then quenching the reaction with with phenylmethylsulfonyl fluoride (5 mM final concentration). Reactions mixtures were diluted with Laemmli buffer, analyzed by polyacrylamide gel electrophoresis in 17% acrylamide gels and detected by staining with Coomassie blue.

extracted from transgenic mouse brains and from transfected cells [39]. However, contrary to PrP^C in crude detergent extracts, the observed in vitro polymerization is specific for Cu^{2+} and does not produce fully proteinase K-protected forms probably due to the absence of other membrane-resident molecule [30,31].

The polymerization process, followed by both turbidity and solubility measurements, requires protein concentrations above 21 ± 4 μM and the saturation of more than 2 sites with Cu^{2+}. Importantly, we find that the formation of insoluble complexes takes place both when Cu^{2+} is presented as a free cation and as a chelate complex. This also rules out artifacts arising from Cu^{2+} instability in aqueous media. Insoluble Cu^{2+}-αBoPrP(24–242) polymers appear as bidimensional meshes consisting of a single layer of protein molecules stabilized by multiple side to side contacts in our AFM analysis. On structural grounds, these side to side contacts and the reduction of the degree of polymerization with increasing protein concentration for a fixed Cu^{2+} concentration support the proposal that the aggregating entity arises from Cu^{2+} cross-linking different αBoPrP(24–242) molecules. In other words, Cu^{2+} can bind to αPrP both intramolecularly and intermolecularly, the mode of binding being determined by the range of the protein concentrations employed.

The crystal structure of the Cu^{2+} complex of the minimal binding site in the PrP molecule (HGGGW) showed Cu^{2+} in a five-fold coordination geometry with the near-equatorial coordinate bonds to the nitrogen of the His imidazole side chain and of the two sequential Gly residues and the amide carbonyl oxygen of the second Gly, and as the axial ligand and an oxygen from a water molecule that is bridged by hydrogen bonding the indole nitrogen of the Trp [20]. This structure, in which the intramolecular Cu^{2+} binding is a short-range, intra-repeat process, has been shown to be compatible with completely Cu^{2+}-saturated, full-length αPrP at low protein concentrations [25]. To allow intermolecular sites we must postulate the existence of an as yet undescribed alternative geometry in which Cu^{2+} 'staples' together different repeats. This interrepeat geometry may either preserve the nature of the coordinating groups, which may belong to different polypeptide chains, or consist of a fully divergent geometry. Taking into account steric impediments and the knowledge obtained from other ligand-induced polymerizing systems such as, for example, that of glutamine synthetase mediated by Zn^{2+} or Cu^{2+}, a different geometry for the interrepeat site seems more plausible. For instance, self-assembly into tubular polymers of the dodecameric glutamine synthetase has been shown to occur by virtue of cation coordination to two sites involving a pair of His residues each belonging to a different polypeptide chains with no structure cost [40].

The finding of Cu^{2+} binding-linked αBoPrP(24–242) polymerization necessitates the recognition of the N-terminal domain of αPrP to be an alternative self-associating domain. However, in contrast to the aggregation mediated by the C-terminal domain, the N-terminal domain polymerizations are linked by ligand binding events and, in the case of that involving Cu^{2+}, do not impair the proteolytic clearance of the prion protein. In fact, we can hypothesize that the regulatory role that the N-terminal domain has in the conversion of PrP^C to PrP^{Sc} is the consequence of its capacity to participate in ligand-linked associations. Spatial coincidence of Cu^{2+}–αPrP bound species at the cell compartments at which exogenous prion recognition and conformationally directed transition occur, opens up the possibility that Cu^{2+}-bound αPrP species are both the receptors as well as the substrates for the conversion of PrP^C to PrP^{Sc}.

Acknowledgements: We thank Francisco Garrido for his extraordinary technical assistance, Dr. D. Laurents and Dr. S. Padmanabhan for critical reading of the manuscript and grammar corrections. This work was supported by Grants BIO2000-1664, BIO2000-P4-174 and BIO2003-0283 from the Ministerio de Ciencia y Tecnología, and by a

NeuroPharma-CSIC contract. M.V. and M.C. are Ramón y Cajal fellows.

References

[1] Basler, K., Oesch, B., Scott, M., Westaway, D., Wälchli, M., Groth, D.F., McKinley, M.P., Prusiner, S.B. and Weissman, C. (1986) Cell 46, 417–428.
[2] Prusiner, S.B. (1998) Proc. Natl. Acad. Sci. USA 95, 13363–133383.
[3] Gasset, M., Baldwin, M.A., Lloyd, D.H., Gabriel, J.M., Holtzman, D.M., Cohen, F., Fletterick, R. and Prusiner, S.B. (1992) Proc. Natl. Acad. Sci. USA 89, 10940–10944.
[4] Pan, K.-M., Baldwin, M.A., Nguyen, J., Gasset, M., Serban, A., Groth, D., Mehlhorn, I., Ziwei, H., Fletterick, R.J., Cohen, F.E. and Prusiner, S.B. (1993) Proc. Natl. Acad. Sci. USA 90, 10962–10966.
[5] Gasset, M., Baldwin, M.A., Fletterick, R.J. and Prusiner, S.B. (1993) Proc. Natl. Acad. Sci. USA 90, 1–5.
[6] Enari, M., Flechsig, E. and Weissman, C. (2001) Proc. Natl. Acad. Sci. USA 98, 9295–9299.
[7] Peretz, D., Williamson, R.A., Kaneko, K., Vergara, J., Leclerc, E., Schmit-Ulms, G., Mehlhorn, I.R., Legname, G., Wormald, M.R., Rudd, P.M., Dwek, R.A., Burton, D.R. and Prusiner, S.B. (2001) Nature 412, 739–743.
[8] Pan, K.-M., Stahl, N. and Prusiner, S.B. (1992) Protein Sci. 1, 1343–1352.
[9] Sulkowski, E. (1992) FEBS Lett. 307, 129–130.
[10] Horshaw, M.P., McDermott, J.R. and Candy, J.M. (1995) Biochem. Biophys. Res. Commun. 207, 621–629.
[11] Brown, D.R., Qin, K., Herms, J.W., Madlung, A., Manson, J., Strome, R., Fraser, P.E., Kruck, T., von Bohelen, A., Schulz-Schaeffer, W., Giese, A., Westaway, D. and Kretzschmar, H. (1977) Nature 390, 684–687.
[12] Stöckel, J., Safar, J., Wallace, A.C., Cohen, F.E. and Prusiner, S.B. (1998) Biochemistry 37, 7185–7193.
[13] Miura, T., Hori-i, A., Mototani, H. and Takeuchi, H. (1999) Biochemistry 38, 11560–11569.
[14] Viles, J.H., Cohen, F.E., Prusiner, S.B., Goodin, D.B., Wright, P.E. and Dyson, H.J. (1999) Proc. Natl. Acad. Sci. USA 96, 2042–2047.
[15] Aronoff-Spencer, E., Burns, C.S., Avdievich, N.I., Gorfen, G.J., Peisach, J., Antholine, W.E., Ball, H.L., Cohen, F.E., Prusiner, S.B. and Millhauser, G.L. (2000) Biochemistry 39, 13760–13771.
[16] Bonomo, R.P., Imperllizzeri, G., Pappalardo, G., Rizzarelli, E. and Tabbi, G. (2000) Chemistry 6, 4195–4202.
[17] Whittal, R.M., Ball, H.L., Cohen, F.E., Burlingame, A.L., Prusiner, S.B. and Baldwin, M.A. (2000) Protein Sci. 9, 332–343.
[18] Cereghetti, G.M., Schweiger, A., Glockshuber, R. and Van Doorslaer, S. (2001) Biophys. J. 81, 516–525.
[19] Jackson, G.S., Murray, I., Hosszu, L.L., Gibbs, N., Waltho, J.P., Clarke, A.R. and Collinge, J. (2001) Proc. Natl. Acad. Sci. USA 98, 8531–8535.
[20] Burns, C., Aronoff-Spencer, E., Dunham, C.M., Lario, P., Avdievich, N., Antholine, W.E., Olmstead, M.M., Vrielink, A., Gerfen, G.J., Peisach, J., Scott, W.G. and Millhauser, G.L. (2002) Biochemistry 41, 3991–4001.
[21] Gustiananda, M., Haris, P.I., Milburn, P.J. and Gready, J.E. (2002) FEBS Lett. 512, 38–42.
[22] Qin, K., Yang, Y., Mastrangelo, P. and Westaway, D. (2002) J. Biol. Chem. 277, 1981–1990.
[23] Garnett, A.P. and Viles, J.H. (2003) J. Biol. Chem. 278, 6795–6802.
[24] Rachidi, W., Mangé, A., Senator, A., Guiraud, P., Riondel, J., Benboubetra, M., Favier, A. and Lehmann, S. (2003) J. Biol. Chem. 278, 14595–14598.
[25] Burns, C.S., Aronoff-Spencer, E., Legname, G., Prusiner, S.B., Antholine, W.E., Gerfen, G.J., Peisach, J. and Millhauser, G.L. (2003) Biochemistry 42, 6794–6803.
[26] Donne, D.G., Viles, J.H., Groth, D., Mehlhorn, I., James, T.L., Cohen, F.E., Prusiner, S.B., Wright, P.E. and Dyson, H.J. (1997) Proc. Natl. Acad. Sci. USA 94, 13452–13457.
[27] Viles, J.H., Donne, D., Kroon, G., Prusiner, S.B., Cohen, F.E., Dyson, H.J. and Wright, P.E. (2001) Biochemistry 40, 2743–2753.
[28] Kramer, M.L., Kratzin, H.D., Schmidt, B., Römer, A., Windl, O., Liemann, S., Hornemann, S. and Kretzschmar, H. (2001) J. Biol. Chem. 276, 16711–16719.
[29] Shaked, Y., Rosenmann, H., Hijazi, N., Halimi, M. and Gabizon, R. (2001) J. Virol. 75, 7872–7874.
[30] González-Iglesias, R., Pajares, M.A., Ocal, C., Espinosa, J.C., Oesch, B. and Gasset, M. (2002) J. Mol. Biol. 319, 527–540.
[31] Hundt, C., Peyrin, J.M., Haik, S., Gauczynski, S., Leucht, C., Rieger, R., Riley, M.L., Deslys, J.P., Dormont, D., Lasmezas, C.I. and Weiss, S. (2001) EMBO J. 20, 5876–5886.
[32] Matsuba, Y. and Takahashi, Y. (1970) Anal. Biochem. 36, 182–191.
[33] Baker, J.O. (1988) Methods Enzymol. 158, 33–55.
[34] Qin, K., Yang, D.S., Yang, Y., Chishti, M.A., Meng, L.J., Kretzschmar, H.A., Yip, C.M., Fraser, P.E. and Westaway, D. (1999) J. Biol. Chem. 275, 19121–19131.
[35] McKinley, M.P., Meyer, R.K., Kenaga, L., Rahbar, F., Cotter, R., Serban, A. and Prusiner, S.B. (1991) J. Virol. 65, 1340–1351.
[36] Chiesa, R., Drisaldi, B., Quaglio, E., Migheli, A., Piccardo, P., Ghetti, B. and Harris, D.A. (2000) Proc. Natl. Acad. Sci. USA 97, 5574–5579.
[37] Chiesa, R., Piccardo, P., Quaglio, E., Drisaldi, B., Si-Hoe, S.L., Takao, M., Ghetti, B. and Harris, D.A. (2003) J. Virol. 77, 7611–7622.
[38] Nunziante, M., Gilch, S. and Schatzl, H.M. (2003) J. Biol. Chem. 278, 3726–3734.
[39] Quaglio, E., Chiesa, R. and Harris, D.A. (2001) J. Biol. Chem. 276, 11432–11438.
[40] Schurke, P., Freeman, J.C., Dabrowski, M.J. and Atkins, W.M. (1999) J. Biol. Chem. 274, 27963–27968.